PACS: 87.50.Gi, 87.53.Wz.

BASIC LAWS OF BOUNDARIES EFFECTS FOR THE ABSORBED DOSE DISTRIBUTION OF ELECTRONS IN THE HETEROGENEOUS MATERIALS

I. Kaluska[**], **V.T. Lazurik**[*], **V.M. Lazurik**[*], **G.F. Popov**[*], **Yu.V. Rogov**[*], **Z. Zimek**[**]
[*]*V.N. Karasin Kharkiv National University, Kharkiv, Ukraine*
[**] *Institute of Nuclear Chemistry and Technology, Warsaw, Poland*
E-mail: popov@univer.kharkov.ua.
Received March 19, 2004.

The anomalies of the absorbed dose distribution of electrons near the boundary of contacting materials at orientation in parallel with incident electron beam were predicted by computer simulation with use the ModeRTL software. Dosimetric experiments were performed on radiation-technological line to validate the theoretical predictions. Heterogeneous targets were irradiated by scanning electron beam with electron energy 10 MeV on moving conveyer. The basic laws predicted by simulation methods on curves of depth-dose distribution of electrons near the boundary of contacting materials with different densities and/or atomic numbers were experimentally confirmed. The physical models for explanation of observed boundaries effects are considered in the report.
KEY WORDS: absorbed dose, electron beam, boundary effects, simulation, experimental validation

At present the electron beam (EB) processing based on electron accelerators are widely used in different industrial radiation technologies, such as sterilization of medical devices; food irradiation; advanced composites modification; wire and cable cross-linking; bulk polymer modification; polymerization of monomers and grafting on monomer onto polymers; tire and rubber pre-cure treatment; purification of water and gas wasters, and others.

For all radiation-technological processes, one of the most important characteristics is the absorbed dose of electrons in an irradiated materials. For each product to be treated in the irradiation facility, there will usually be a minimum dose limit D_{min} to obtain the desired effect and a maximum dose limit D_{max} that the product can tolerate without degradation in quality [1]. Value of an absorbed dose of electrons necessary for realization of the EB processing, the required level of dose uniformity ratio (DUR = D_{max}/D_{min}) in volume of the irradiated product determine efficiency and productivity of the technological process.

In various EB technologies, DUR essentially depends on the boundary anomalies in depth-dose distributions, which appear under irradiation of heterogeneous targets [2,3]. For example in practice, such boundary anomalies appear under irradiation by EB of contacting materials (solid/liquid) with different densities and/or atomic numbers, near the boundary of irradiated materials with package and with air, on the boundary of irradiated materials with materials of body dosimeter, etc. Theoretical and practical investigations of the boundary anomalies for depth-dose distributions and interpretation of dosimetric results are the actual tasks for dosimetry of industrial radiation technologies [3,4].

Results of simulation and measurement of the features for the absorbed depth-dose distribution near the boundaries of two contacting materials with different densities and/or atomic numbers irradiated with an electron beam (EB) are discussed in the report.

The numerical investigations of a dose distribution in heterogeneous targets irradiated on radiation-technological lines (RTL) by a scanning electron beams on moving conveyer were carried out with use of ModeRTL software [2,3,5,6]. The ModeRTL (Modeling of the Radiation-Technological Line) software was developed to simulate radiation processes and calculate the absorbed dose, temperature, and charge distributions within products irradiated by a scanning electron beam with electron energy range from 0.1 to 25 MeV on industrial RTL. The ModeRTL uses in the unified calculation scheme for the transport of electrons in materials of different calculation methods, such as analytical, semi-empirical, and precise - method Monte Carlo. It provides high veracity of simulated results and decisions accepted on this base.

Validation of the depth-dose distributions predictions with dosimetry was fulfilled on the industrial RTL with linear electron accelerator LAE 13/9 at the INCT, Warsaw [7]. Simulation and measurement of boundary effects for the depth-dose distribution were carried out for targets irradiated by scanning EB with energy 10 MeV on moving conveyer.

EB FACILITY AND SIMULATION MODEL

The geometrical models for typical EB radiation facility that were used for simulation of EB processing by the ModeRTL program and often are used in practice are shown in Figs. 1(a) and (b). The model on the Fig. 1(a) is close to the industrial RTL with linear electron accelerator LAE 13/9 at the INCT, Warsaw, where dosimetric investigations of boundary effects were carried out. The ModeRTL program takes into account in detail a construction of the RTL and requirements to process of irradiation in each specific radiation technologies. A source of electron beam, a scanner, a conveyor line, an irradiated target and a package are considered in uniform self-consistent geometrical and physical models. Figs. 1(a) and (b) represent two geometrical models of EB facility which forms a dose field by a scanning EB into heterogeneous target placed on moving conveyer. The gap between outlet window of accelerator and the incident surface of irradiated target is filled with air. Figs. 2 (a), (b), (c), and (d) demonstrate the different models for irradiated target within package which are used by the ModeRTL program for simulation EB processing.

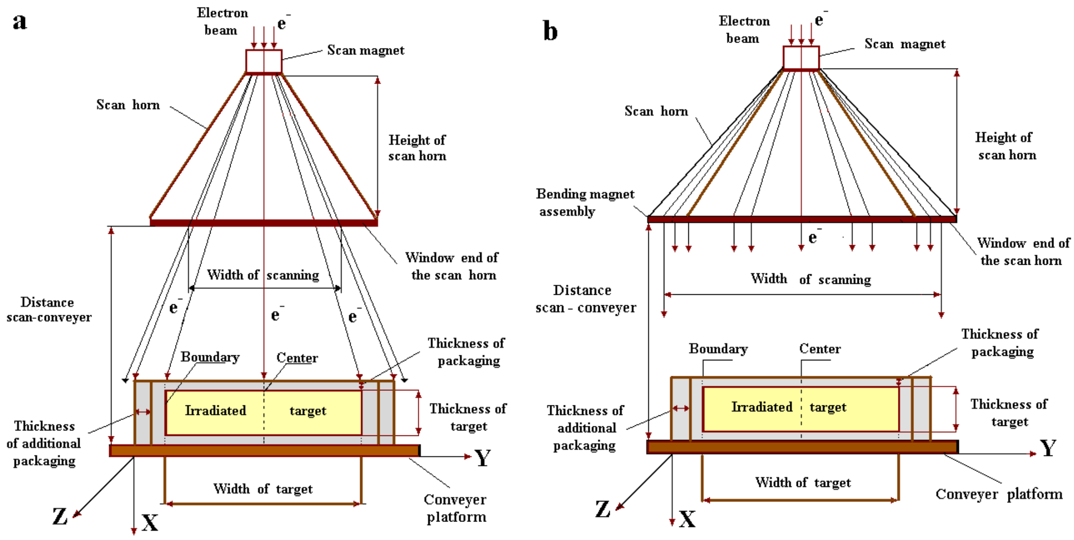

Fig.1. Schemes of EB radiation facility with target and package box placed on moving conveyor.
a) The target irradiated by EB with triangular scanning.
b) The target irradiated by EB with non-diverging (parallel ray) scanning.

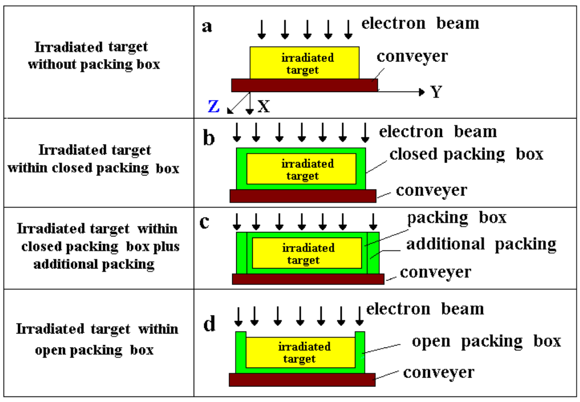

Fig. 2. Geometrical models of irradiated targets and packing placed on moving conveyer and irradiated by EB.

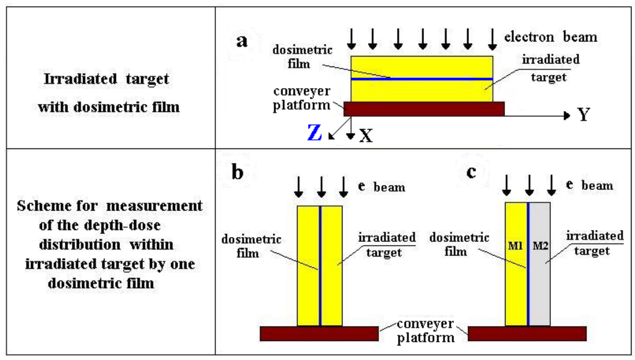

Fig.3. Models of irradiated target with dosimetric film inserted within materials.

Figs. 3 (a), (b) and (c) demonstrate the geometrical models of irradiated targets with dosimetric film inserted in perpendicular Fig. 3 (a) or in parallel Figs. 3 (b) and (c) with electron beam into irradiated material. Simulation of the depth-dose distribution in dosimetric film is carried out with consideration of the boundary effects between the dosimetric film and the irradiated targets. Model on the Figs. 3 (b) and (c) allows to simulate and measure the complete curve of the depth-dose distribution by one dosimetric film.

Simulation of EB dose distributions in an irradiated heterogeneous target was fulfilled by Monte Carlo (MC) and analytical methods in two-dimensional (2-D) geometrical model. At implementation of the simulation MC methods the specially designed schemes which allow to reduce a running time for obtaining of the end results in about hundreds time were applied [6].

The 2-D dose distribution in the target is represented as function of two coordinates - of the target depth (axis X) and the target width along scan direction (axis Y). Conveyer moves along axis Z. Such conditions are realized in many cases for EB processing when the target is irradiated at one- and double-sided on the moving conveyer.

The heterogeneous target on a conveyer line was represented as a set of parallelepipeds unlimited on length along a motion of the conveyer (axis Z). It is supposed, that the parallelepiped sides are oriented only in parallel of each other, and the material of each element of the target (represented as separate parallelepiped) is homogeneous. Dose fields in a plane of scanning of an electron beam (plane XY) were calculated. Depth-dose distributions (depth is measured from the incident surface of target along an axis X perpendicular to axis Y) were compared on various distances from a boundary of materials with different densities and/or atomic numbers.

Dosimetric film was modeled as thin sheet unlimited on length inserted in parallel axis of EB between the contacting homogeneous materials in plane XZ (see Figs. 3(b) and (c)). Simulation of boundary effects for the depth-dose distributions near the boundary of irradiated materials with air was performed according to the target model on Fig. 2(a). Modeling of an EB transport from outlet window of accelerator to the incident surface of an irradiated target takes into account the scattering of electrons in an air gap.

THEORETICAL STUDY OF BOUNDARY EFFECTS

Two type of the heterogeneous targets consisting of two blocks were chosen for an illustration of some theoretical predictions, obtained on the basis of results analysis of computer experiments. In the first target 1, blocks of contacting materials have different chemical composition and densities (ρ_i). For example, the target 1 can include block of homogeneous polyethylene (PE) with density of 0.94 g/cm^3 and effective atomic number Z_{ef} = 4.76 and aluminum (Al) block with density of 2.7 g/cm^3 and atomic number Z = 13. For these materials: ρ_{Al}/ρ_{PE} = 2.87, Z_{Al}/Z_{PE} = 2.73. In the second target 2, blocks of contacting materials have identical chemical composition and different densities. For example, such target can be easily implemented with use of homogeneous (PE density of 0.94 g/cm^3) and granules (PE1 bulk density of 0.3 g/cm^3) polyethylene. The geometrical parameters of a targets were chosen so that the curves of depth-dose distribution at center of blocks corresponded to an extreme case of a semi-infinite target. It is implemented when the sizes of blocks greater than r_0 – continuous slowing-down approximation range of electrons in material of the block. For polyethylene and electron energy 10 MeV value r_0 = 4.81 g/cm^2, for Al - r_0 = 5.85 g/cm^2 [8]. Targets on moving conveyer were irradiated by scanning electron beam with electron energy 10 MeV and the energy spread on the half of distribution curve ± 2.5%.

The transport and interaction of primary and secondary electrons with material of target was simulated by a method Monte Carlo. The dose value was determined as the ratio of average value of deposited energy in a spatial bin (with the sizes $0.01r_0$•$0.01r_0$) to mass of this bin. The dose distribution near the boundary of contacting materials was determined by averaging of a dose in a direction of perpendicular boundary of materials on the bin size Y_i = 0.01 r_0.

The simulation results for electron depth-dose distribution in the target 1 and target 2 performed by an analytical and a Monte Carlo methods are shown in Figs.4 (a) and (b) respectively. Fig. 4(a) represents the depth-dose distributions at center of PE block (curve 1) and near the boundary of PE block with Al block (curve 2). Curve 3 represents the depth-dose distribution near the boundary of PE block with Al block in case when Al block has identical density with PE block, i.e. $\rho_{Al} = \rho_{PE}$ = 0.94 g/cm^3.

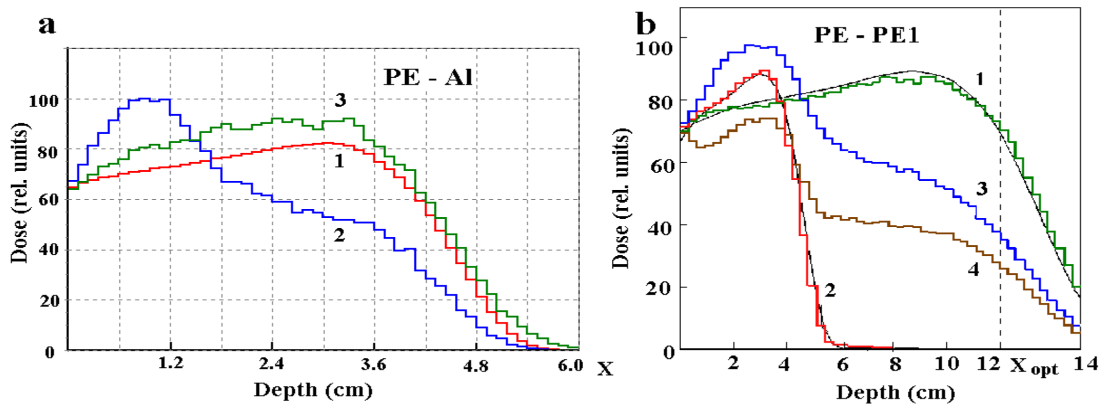

Fig. 4. Depth-dose distribution in the target.

a) a) The target 1 consists of contacting PE and Al blocks:
1 - dose distribution at center of PE block; 2 – dose distribution near the boundary of PE block with Al block (density 2.7 g/cm^3);
3 - dose distribution near the boundary of PE block with Al block (density 0.94 g/cm^3).

b) The target 2 consists of two polyethylene blocks with different density: 1 and 3 - dose distributions at center and near the boundary of PE1 block with density 0.3 g /cm^3 respectively; 2 and 4 – dose distributions at center and near the boundary of PE block with density 0.94 g /cm^3 respectively. Histograms - results of calculations by a method Monte Carlo, solid curves - results of calculations by a semi-empirical model.

In this case the materials of contacting blocks have only different chemical composition which characterized by their effective atomic numbers Z_i. The root-mean-square deviation between shape of dose distribution for the center of homogeneous PE (curve 1) and shapes of dose distributions on the boundaries of PE with Al (ρ_{Al} = 2.7 g/cm^3) (curve 2) is 37%, and of PE with Al (ρ_{Al} = 0.94 g/cm^3) (curve3) is 12%. Therefore, the boundaries effects for the depth-dose distribution of contacting materials are mainly determined by difference in materials density.

Let's note that dose anomalies which appear near the boundaries of two materials with different atomic numbers are well known. As a rule, the consideration of these effects is performed for a case of normal incidence of an electron beam and at a uniform irradiation of a boundary of contacting materials, i.e. in one-dimensional model. In this case, the influence of density of the contacting materials on value of boundary effects can be neglected.

Fig. 4(b) represents the depth-dose distributions for two contacting materials with identical chemical composition and different densities: homogeneous (PE density of 0.94 g/cm^3) and granules (PE1 bulk density of 0.3 g/cm^3) polyethylene. The vertical line in the Fig.4 (b) corresponds to an optimum thickness X_{opt} of irradiated PE1 block where the exit dose equals the entrance dose (see curve 1). Range of the target depth from X=0 to X=X_{opt} represents the basic interest for practice. For a heterogeneous target near the boundary of two materials with different density the value of an absorbed dose for thickness X_{opt} is much less, than in a homogeneous material (see curve 3).

Figs. 5(a) and (b) represent results simulation of 3D view for depth-dose distributions in the target consisting of PE block with density 0.94 g/cm^3 inserted in open box made of PE1 with density 0.3 g /cm^3 (Fig. 5(a)), and - in the target consisting of PE1 block with density 0.3 g/cm^3 inserted in open box made of PE with density 0.94 g /cm^3 (Fig. 5(b)). Targets within box were at one-sided irradiated by a scanning EB with energy 10 MeV on moving conveyer. Dose distributions 2 and 4 at center and near the boundary of PE block with density 0.94 g /cm^3 respectively in the Fig.4(b) correspond 3D view for depth-dose distribution in the Fig.5(a). Dose distributions 1 and 3 for PE block with density 0.94 g/cm^3 in the Fig.4(b) correspond 3D view for depth-dose distribution in the Fig.5(b).

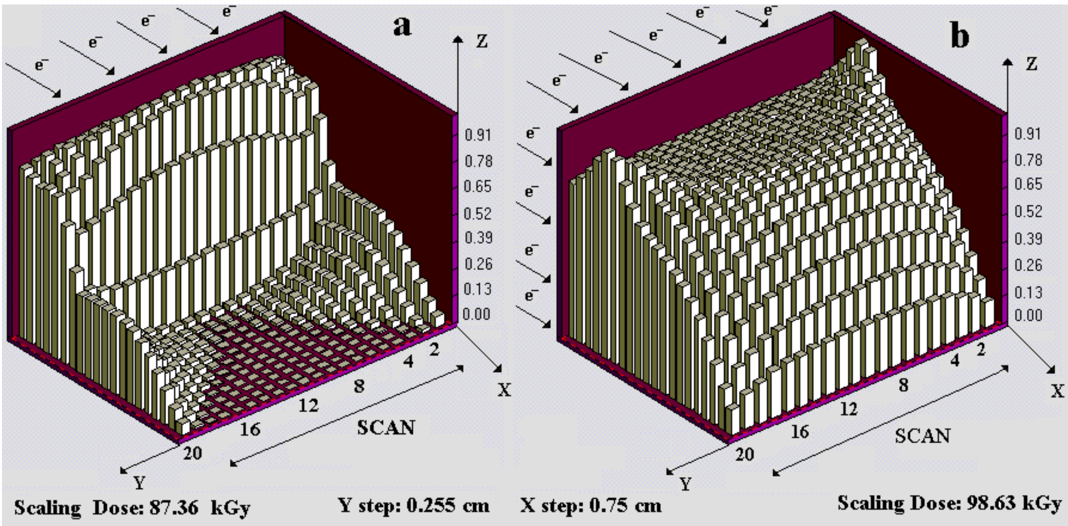

Fig. 5. 3D view for depth-dose distributions in the target.

a)The target consists of PE block inserted in open box made of PE1.

b) The target consists of PE1 inserted in open box made of PE.

As it is seen from Figs.4(a), (b) and Figs. 5(a), (b), the depth-dose distribution near the boundaries of the contacting of materials with various density can strongly differ in the shape from the depth-dose distribution on considerable distances from boundary in each of contacting materials.

The natural supposition appears at visual comparison of curves represented in Figs.4(a), (b), that the depth-dose distribution near the boundaries of materials with various density can be described as a linear superposition of the depth-dose distribution in unlimited layers of contacting materials. It is equivalent of the elementary theoretical model in which it is supposed, that the dose in a boundary layer is determined by radiation flows coming out of two not interacting semi-infinite mediums.

Some embodying of this model is presented in Fig.6. In this figure the data for curves 1, 2, and 3 correspond to the data presented in Fig.4. The dash curves 4 and 5 are obtained as a linear superposition of data presented as curves 1 and 2: $D_b(X) = A \bullet D_1(X) + B \bullet D_2(X)$, where $D_1(X)$, $D_2(X)$ - dose on depth X in material of the first and second blocks respectively, A, B - superposition parameters. The curve 4 is obtained at A=0.5, B=0.5. The curve 5 is obtained by fitting of $D_b(X)$ by a least-squares method to the data presented to a curve 3 at a variation of parameters A and B. As a result of fitting, the parameters A and B have the following values: A=0.65, B=0.51.

As it is seen from Fig. 6, the shape of curves 3 and 5 essentially differs even at optimum adjustment of model parameters for not interacting mediums. In a considered case (high energies of electrons and small effective atomic number of material) the reflectivity of electrons are not so small only for sliding angles of incidence. It is possible to conclude about the essential contribution of electrons which move along boundary and repeatedly intercross it to process of boundary effects formation.

Comprehensive analysis of simulation results of the depth-dose distribution of electrons near the boundary of two materials at orientation in parallel with incident electron beam allows to formulate the following basic laws for an electron dose distribution near the boundaries of the contacting materials with different density and/or atomic number:

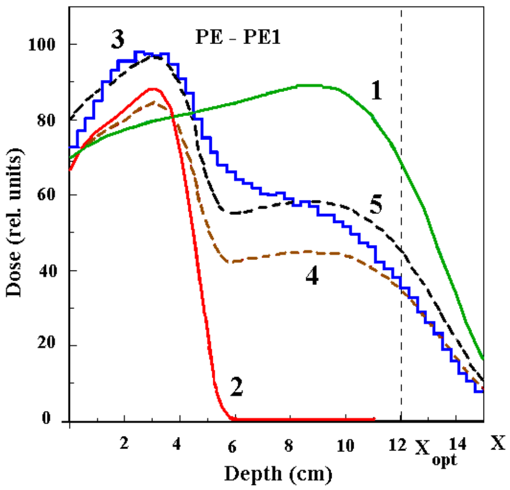

Fig. 6. Depth-dose distribution in the target consisting of two polyethylene blocks with different density.
1 and 3 - dose distributions at center and near the boundary of PE1 block with density 0.3 g/cm^3; 2 – dose distributions at center of PE block with density 0.94 g/cm^3; 4 - dose distribution near the boundary of PE block calculated as a linear superposition of the dose distributions in unlimited layers of contacting materials, superposition parameters A=0.5, B=0.5; 5 - dose distribution near the boundary of PE block calculated as a linear superposition of the dose distributions in unlimited layers of contacting materials with using a least-squares method, A=0.65, B=0.51.

1. The boundaries effects for the electron depth-dose distribution of contacting materials with different density and/or atomic number are mainly determined by difference in materials density.
2. Depth-dose distribution of electrons near the boundaries of the contacting materials with different density differ in the shape from a depth-dose distribution in semi-infinite target for each of contacting materials.
3. The values of doses near the boundary of two materials which differ only in density coincide on the incident surface of a target and can differ in depth of a target.
4. The value of an absorbed dose in material with smaller density is greater than in material with greater density on all depth of an irradiated target.
5. Maximal values of an electron dose near the boundary of the contacting materials with different density can exceed maximal values of a dose in semi-infinite target for each of contacting materials.
6. The local minimum in depth-dose distribution can appear on small distances from a surface of a target in material with greater density.
7. Depth-dose distribution of electrons near the boundaries of contacting materials with different density has the similar shape on considerable depth from the incident surface of a target.
8. The shape and value of the depth-dose distribution of electrons near the boundary of contacting materials with essentially different densities are very sensitive to the orientation of lateral face of irradiated materials relatively to axis of electron beam, as well as to angular spread of EB.

The theoretical analysis of mentioned above general laws allows draw a conclusion about a determinative role of electrons, which move along boundary, in the process of formation of a boundary effects for depth-dose distribution. It means, that performing simulation of trajectories of electrons in irradiated target, the special attention should be given to the transverse displacements of an electron.

Let's note that the cases to appearance of artifacts are known at interpretation of calculated values of a dose obtained for boundary areas due to of errors in simulation of transverse displacements of an electron [9].

It is important for development of theoretical models to utilize an experimental validation of basic laws of boundary effects predicted on the basis of computer simulation of an irradiation process with use of the ModeRTL software. As it is well known, that quality of an irradiation process in radiation technologies according to the ASTM Standard 1649-94 is determined by values of the dose limits [1]. The minimum dose limit D_{min} to obtain the desired effect and a maximum dose limit D_{max} to avoid product degradation usually exist for each product to be treated in the EB irradiation facility. Therefore, the practical recommendations and conclusions obtained on the basis of the mentioned above basic laws for dose distribution near the boundaries of heterogeneous targets are important for radiation technologies. Thus, the theoretical predictions require experimental validation on actual RTLs.

EXPERIMENTAL

The experimental investigations of the absorbed depth-dose distribution of electrons near the boundary of two materials with different density and/or effective atomic number, irradiated by a scanning electron beam with energy 10 MeV on moving conveyer were fulfilled. The absorbed dose for irradiated materials was delivered in the range of 30-60 kGy. The experiments were performed on the radiation facility with linear electron accelerator LAE 13/9 at the Institute on Nuclear Chemistry and Technology in Warsaw.

Validation of the theoretical predictions for boundary anomalies of the depth-dose distributions of electrons in heterogeneous targets with dosimetry was performed with the use of two types of models for the targets: two-component targets, in which a thin dosimetric film was inserted into homogeneous materials (see Fig. 3(b)); three-component targets, in which a thin dosimetric film was inserted between two different materials (see Fig. 3(c)).

Dose effects near the boundary of two contacting materials with different density and atomic number such as Al with density 2.7g/cm^3, high density polyethylene (PE) block with density 0.94 g/cm^3, PE1 granules with bulk density 0.66 g/cm^3, and wood with density 0.44 g/cm^3 were investigated. The materials were represented as parallelepipeds at which the contacting boundaries are in parallel with an axis of electrons beam.

The geometrical sizes of each blocks along an axis of electron beam (axis X), along a direction of scanning (axis Y) and a direction of conveyer travel (axis Z) were chosen from a requirement $x_i, y_i, z_i \geq r_0$, where r_0 is continuous slowing-down approximation range of electrons with energy 10 MeV in each material. Heterogeneous target from two, three or four contacting materials was placed in a carton box with the size 340x320x200mm, which was filled to a level of X=150 mm with granules of high density PE. The box with targets was placed on a foam plate by thickness of 40 mm in a standard Al box with the size of 560x480x200 mm and walls thickness of 1 mm. Such boxes usually use in practice for sterilization of medical devices.

One variant of setup for heterogeneous target with dosimetric films on a conveyer platform is shown in Figs.7 (a) and (b). Fig. 7(a) is a top view of the target consisting of four blocks of contacting materials. Fig. 7(b) is a view of the target at section A-A in plane of an EB axis. Three dosimetric films in shape of strips with 8mm wide and 150mm long were inserted side-by-side between all contacting blocks in parallel with EB axis.

There are five boundaries between contacting materials on Figs. 7 (a) and (b) where dosimetric films were inserted: PE granules - wood (1), wood - wood (2), wood - Al (3), Al - Al (4), and Al - PE granules (5).

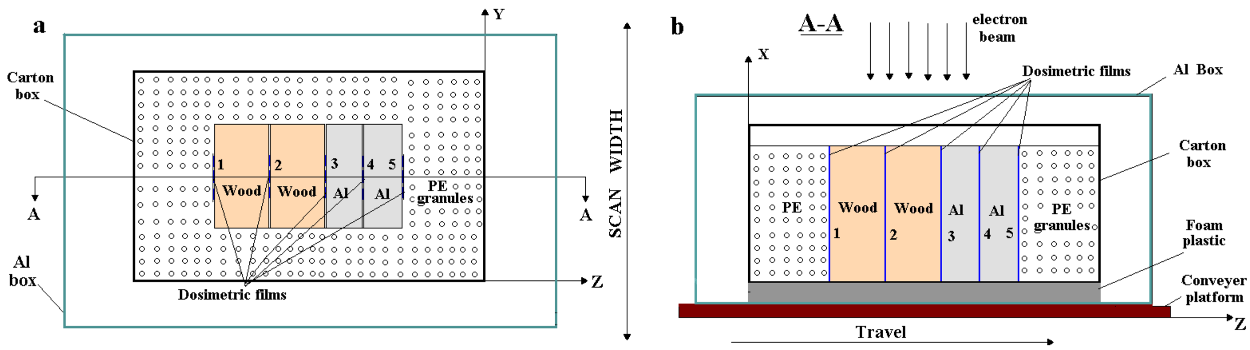

Fig. 7. Experimental setup of heterogeneous target with dosimetric films on a conveyer platform.

a) Top view of the target consisting of four blocks of contacting materials.

b) Target view at section A-A.

Another types of boundary effects for depth-dose distribution, which realized in practice, were investigated on the boundaries of target materials with walls of Al box and target materials with air. Position of irradiated materials in Al box for such experiment is represented in Fig.8. There are four boundaries where dosimetric films were inserted: wood - wood (1), wood - air (2), wood - middle of front wall of Al box (3), wood - middle of side wall of Al box (4). On the boundary of wood - air (2), three dosimetric films were close placed side-by-side on the lateral surface of wooden block in parallel with EB axis.

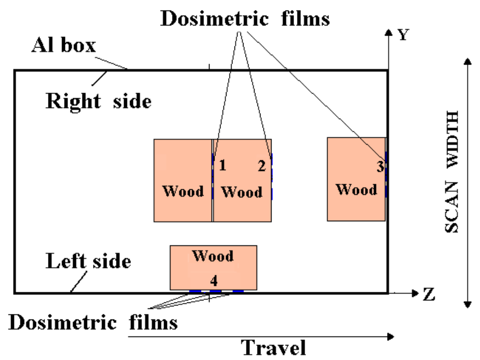

Fig.8. Experimental setup of heterogeneous target with dosimetric films for investigations of dose distributions on the boundary of target materials with walls of Al box and with air.

Cellulose Triacetate (CTA) dosimetric film (FTR-125) with thickness 0.125 mm and density 1.32 g/cm^3 was used for measurement of a depth-dose distribution. The FDR001 spectrophotometer in automatic regimes was used for reading of optical density on wavelength 280 nm from CTA strip films. Dosimetric films were inserted between contacting blocks in parallel with axis of electron beam. Such geometry of irradiation allows to obtain the depth-dose distribution on the boundary of contacting materials by one dosimetric film.

The heterogeneous materials were irradiated by a scanning electron beam with energy 10 MeV, average beam current 0.34 mA, scan width 46 cm, conveyer speed 0.128 m/min, angular spread 3 degree. Three PVC (polyvinylchloride) dosimetric sheets inserted perpendicular along electron beam axis on 3 various distances 14, 31 and 46 cm from outlet window of electron accelerator were used for estimation of angular spread of electron beam. Dosimetric sheets with thickness of 0.25 mm were irradiated by electron beam in stationary regime. Angular spread was determined on value of electron beam size along axis Y which was measured by dosimetric sheets.

RESULTS AND DISCUSSION

Dose distributions in CTA dosimetric films placed between identical materials

The experimental results related with value and profile of the dose distributions in CTA dosimetric films inserted between identical materials are presented in Figs. 9 (a), (b). Results of the specially carried out dose distribution measurements in CTA films inserted in the standard dosimetric Al wedge marked as points and obtained with use of the ModeRTL software (histograms) are presented in Fig. 9(a). The relative accuracy of these data did not exceed 5 % for values of doses grater than 10 kGy. The uncertainty of the depth value of all curves is 0.04 cm and the average size in each point is 0.03 cm. The ModeRTL software provides effective simulation by a Monte-Carlo method of the depth-dose distribution in thin dosimetric films inserted between two blocks that are made of identical material. Results of Monte Carlo simulation of the depth-dose distributions in homogeneous materials (histograms with points +) and obtained by semi-empirical model for semi-infinite medium (dash line) are presented for comparison in Fig. 9(a).

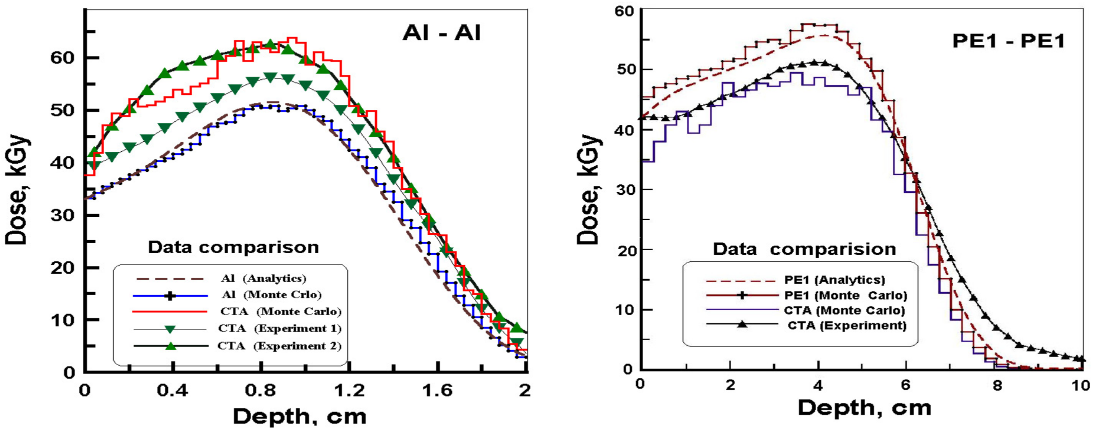

Fig. 9. Depth-dose distribution in the targets.

a) The target consists of two Al blocks. Histograms - results of calculations by a method Monte Carlo of the dose distribution in Al blocks (points +) and in CTA film inserted between two Al blocks; Dash lines – dose distribution calculated with the use semi-empirical model at the center of Al blocks. Experimental results for dose distribution measured by CTA film inserted between two Al blocks (Experiment 2) and inserted in Al wedge (Experiment 1) are shown by points.

b) The target consists of two blocks PE1 with density 0.66 g/cm^3. Histograms - results of calculations by a method Monte Carlo of the dose distribution in PE1 blocks (points +) and in CTA film inserted between two PE1 blocks; Dash lines – dose distribution calculated with the use semi-empirical model at the center of PE1 blocks. Experimental results for dose distribution measured by CTA film inserted between two PE1 blocks are shown by points.

The validation and editing of the input data for the ModeRTL program were carried out by comparison of the depth-dose distributions simulated by Monte-Carlo method in targets consisting of two Al blocks with experimental results for dose distribution measured by CTA film in standard dosimetric Al wedge (Fig. 9 (a), Experiment 1) [1]. As it is seen from Fig. 9 (a), the ratio of calculated values of dose in CTA film to dose in Al near the incident surface of target (X=0, see values in the first cells of two histograms) corresponds to the ratio of values of dose measured by dosimetric wedge (Experiment 1) to calculated values of dose in Al (histogram with points +) on any depth in the target.

As this ratio is close to value 1.1 and that it corresponds to the ratio of electron stopping powers of materials CTA to Al, it is possible to consider that input data for carrying out of calculations are given correctly. Difference of dose profile in CTA film from dose profile in the target material (Experiment 2) are determined by two factors: by change of dose profile due to differences of stopping powers of materials (first factor) and change of dose profile due to differences of materials density (second factor). The smaller density and greater stopping power of CTA film material relatively Al corresponds to a case, when both factors work in one direction, that lead to considerable excess of a dose distribution in CTA films relatively a dose in Al (greater than 20 %).

It should be note also, that difference in density of the film material and the target materials lead to appreciable distortion of a dose profile in a film (compare curves of a dose - measured by Al dosimetric wedge (Experiment 1) and calculated (or measured) in CTA films). It essentially distinguishes a case, when there is a difference in densities of contacting materials from a case, when there is a difference only in stopping powers of material.

The conclusions formulated on the basis of the visual analysis presented on Fig. 9(a) are agreed with experimental and simulation results for PE1 granules (see Fig. 9 (b)). The ratio of a stopping power of CTA film material to a stopping power of PE is less than 1 and density of CTA film material more than PE density. Therefore, differences of a dose profile in a CTA film from a dose profile in bulk PE1 are determined by two factors, as well as for a case of CTA film in Al. However, in this case, action of the factors is opposite and the values difference of doses in CTA film and in bulk PE1 less on an absolute value and have an opposite sign.

Experiment with wooden blocks has shown that the ratio of a stopping power of CTA material to a stopping power of wooden material is very close to 1. Differences of a dose profile in CTA film from a dose profile in a wooden material completely are determined by difference in densities of their materials, i.e. only by one of two factors.

On the basis of comparison of experimental and calculation data in Al, PE granules, and wooden blocks it is possible to made the conclusion that ModeRTL software allows to ensure the correct forecast and interpretation of observed data for dose distributions in a homogeneous material measured by dosimetric films inserted in parallel with electron beam.

Dose distributions near the boundary of materials with different density and atomic number

Dose effects near the boundary of two contacting materials with different density and atomic number such as Al with density 2.7g/cm^3, high density polyethylene (PE) block with density 0.94 g/cm^3, PE1 granules with bulk density 0.66 g/cm^3, and wood with density 0.44 g/cm^3 were studied. The simulation and experimental results related with value and profile of the dose distributions in CTA dosimetric films inserted between two blocks at various combinations of materials (Al, PE, wood) are presented in Figs. 10 (a) and (b). Results of Monte Carlo simulation (histograms) of the depth-dose distributions on the boundary of two contacting blocks consisting of different materials and obtained by semi-empirical model for semi-infinite medium (solid line) are presented in Figs. 10 (a) and (b). The bins depth of averaging dose in direction of perpendicular boundary of blocks for each material is 0.01 r_0. For electron energy 10 MeV in Al - r_0=5.85 g/cm^2, in PE - r_0=4.81 g/cm^2, in wood - r_0=5.27 g/cm^2. X_{opt} is the optimum target thickness for PE and wooden blocks at one-sided irradiation respectively.

General labels on Figs.10(a) and (b) specify a combination of materials between which the CTA dosimetric films were inserted. First index in the labels on dose distribution curves show to which from two contacting materials this curve concerns. Experimental results for depth-dose distribution measured by CTA film inserted between materials are shown by points. The relative uncertainty of experimental data did not exceed 5% for values of doses greater than 10 kGy. The uncertainty of the depth value of all curves is 0.125 cm and the average size in each point is 0.1 cm. The requirements for experiments and computer modeling were chosen so that in the selected range of depths the relative deviation of measuring was no greater than 5 %, relative root-mean-square statistical error was no greater than 5 %.

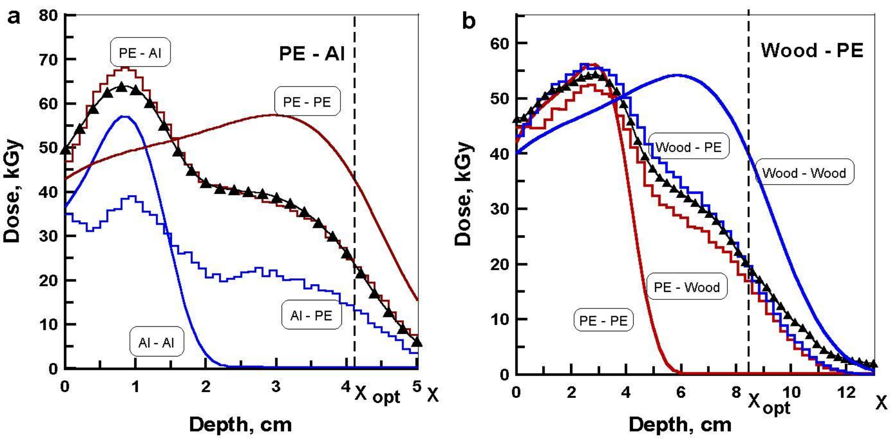

Fig. 10. Depth-dose distribution in the heterogeneous targets.

a) The target consists of PE and Al blocks (PE density 0.94 g/cm^3).

b) The target consists of wooden and PE blocks (wood density 0.44 g/cm^3).

Histograms – results of calculations by a method Monte Carlo of the depth-dose distribution near the boundary of Al, PE, and wooden blocks; Solid curves – depth-dose distribution at the center of Al, PE, and wooden blocks calculated with the use semi-empirical model.

As it is seen from Figs.10(a) and (b) in the selected range of target depths the measurement results are satisfactorily agreed with results obtained on the basis of simulation of an irradiation process by a Monte-Carlo method. The above results concerned to a case when the sizes of the contacting materials in a direction perpendicular to a boundary of target are great and it is possible to suppose a target by unlimited.

The cases when one of the contacting layers has relatively small size are of interest for practice. In these cases, the use of the ModeRTL software for obtaining simulation data is valid. Because, the experimental validation of correctness for simulation of a dose profile was obtained for two limiting cases - very much thin material layers (films, see Figs. 9(a) and (b)) and thick blocks (unlimited medium, see Figs. 10(a) and (b)).

It is possible to conclude, that basic laws of boundary effects which were described in items 1,2,4,5,7 ("Theoretical study of boundary effects") obtained theoretically with using the ModeRTL software are experimentally validated. The established fact of strong distortion of a dose profile in thin dosimetric film (see Figs. 9(a) and (b)) specifies necessity of modernization of measurement principles for experimental validation of items 3 and 6 for the list of basic laws of boundary effects.

The features of dose distributions near the boundary of irradiated materials with package and with air

The boundaries effects on the depth-dose distribution at irradiation with EB of contacting materials for two practical cases are considered in this chapter. In the first case, the width for one of contacting materials Y_i in plane XY of EB scanning is essentially less than $(r_o)_i$ for this materials, i.e. $Y_i << (r_o)_i$. For example, such conditions realized on the boundary of irradiated materials with package. In the second one, the density for one of contacting materials ρ_1 is essentially less than density of another material, i.e. $\rho_1 << \rho_2$. In practice, such conditions are realized on the boundary of solid/liquid materials with air. Geometrical model of irradiated target for simulation and experimental investigation of such boundaries effects is shown in Fig.8. Thickness of Al wall is 1 mm, wooden block has size 15x14x12 cm, 15x14 cm in plane XZ. Three dosimetric CTA films were inserted side-by-side between wooden blocks and walls of Al box in parallel with EB axis.

Fig.11(a) represents the results of Monte Carlo simulation of the depth-dose distribution on the boundary of wooden blocks with walls of Al box. Curve 1 is the depth-dose distribution in homogeneous wooden material. Curve 2 is the depth-dose distribution in the wooden block on the boundary with the middle of front wall of Al box, curve 3 - on the boundary of wooden block with the middle of side wall of Al box.

Fig 11(b) represents the results of experimental measurements of boundaries effects for the depth-dose distribution in wooden blocks irradiated by scanning EB. Geometry of irradiated targets for simulation and experimental was identical. Curve 1 is the dose distribution measured in the center of homogeneous wooden material. Curves 2 and 3 represent of experimental dose distribution in wooden blocks on the boundary 3 with the middle of front wall (curve 2) and with the middle of side wall (boundary 4, curve 3) of Al box respectively (see Fig.8).

Al box for movement of materials through the field of EB irradiation have two different boundaries with respect to formation of an absorbed dose in an irradiated material, which contacts with box walls. The first type of boundary is located in plane XY of scan EB on the front walls of the box relatively direction of conveyer motion, the second one is located in plane XZ on the side walls.

The difference of the shapes for depth-dose distribution (see Figs. 11(a) and (b)) on the boundaries 3 and 4 (see Fig.8) is determined by difference of the angle of incidence for EB on the boundaries in plane XY of EB scanning. On the boundary 4, EB irradiation of the wooden block contacting with middle of side wall of Al box is performed at angle 10 degree in respect to EB axis in plane of scan XY, on the boundary 3 - at angle ~ 0 degree.

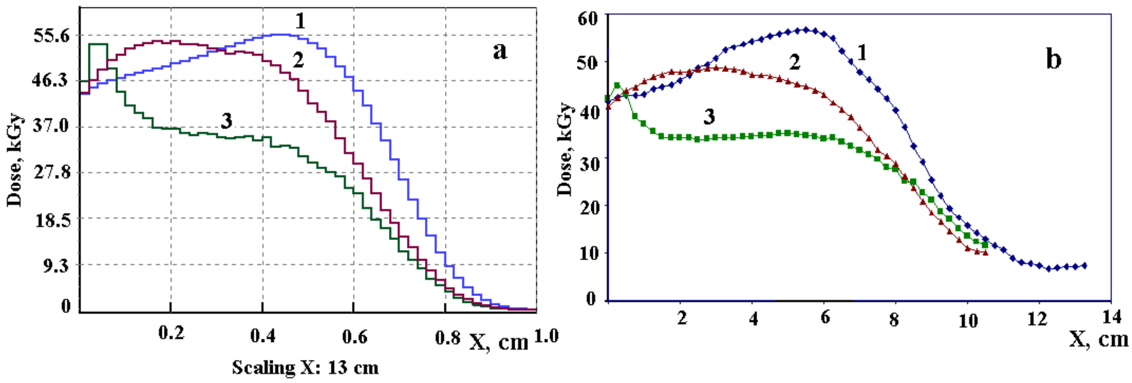

Fig. 11. The depth-dose distributions on the boundary of wooden blocks with walls of Al box.

a) Simulation results. b) Experimental results.

1- dose distribution in homogeneous wooden material; 2- dose distribution in the wooden block on the boundary with the middle of front wall of Al box; 3 - dose distribution on the boundary of wooden block with the middle of side wall of Al box.

The analysis of the depth-dose distribution on the Figs. 11(a) and (b) demonstrate a good agreement of the shapes of depth-dose distributions for theoretical predictions and experimental validation and a satisfactory agreement in absolute values. Greater value of the experimental absorbed dose at the end of electron range in wooden material in comparison with simulation results (see Figs.11(a) and (b)) is determined by influence of back scattered electrons from materials of conveyer platform.

The influence of the target inclination on angle β in respect to electron beam axis in plane of scanning XY (see Fig.12.) as well as angular spread of electron beam on the depth-dose distributions of the boundary of wooden block with air were investigated by modeling with the program ModeRTL. Geometrical model for the target inclination on angle β in respect to EB axis in plane XY is shown in Fig.12. As it is seen from Fig.12, the right and left lateral sides of target materials are in different conditions of irradiation by electron beam. The right lateral side of target is partly highlighted by electron beam, the left lateral side of target is partly shaded for electron beam. So, the forming of absorbed dose on the left and right boundaries of target materials is different.

Results of Monte Carlo simulation of the depth-dose distributions on the boundary of wooden block with air are presented in Fig. 13(a). Curve 1 is the depth-dose distribution in homogeneous wooden material, curve 2 is the depth-dose distribution in the wooden block near the boundary with air and without the block inclination (β=0 degree). Curve 3 is the depth-dose distribution in the wooden block near the left lateral side (shaded side) of target under inclination

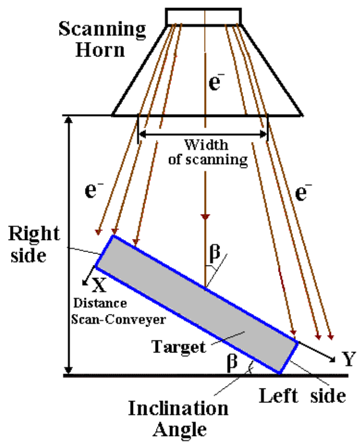

Fig.12. Geometrical model for the target inclination on angle β in respect to EB axis in plane XY. Right lateral side - highlighted side, left lateral side - shaded side.

angle β=3 degree, curve 4 is the depth-dose distribution in the wooden block near the right lateral side (highlighted side) of target under inclination angle β=3 degree. Curves 1,2,3,4 for the depth-dose distributions were calculated for electron beam with angular spread of 3 degree. Curve 5 is the depth-dose distribution in the wooden block near the boundary with air irradiated by electron beam with angular spread of 6 degree under inclination angle of the target β = 0 degree.

For the center of the wooden block under its inclination in the range of angles β = 1-3 degrees, and for electron beam with angular spread in the range of angles 3-6 degrees, root-mean square deviation for the shape of dose distributions does not exceed 2%. Root-mean square deviations between curves 2, 3,4, and 5 for the shape of dose distributions are in the range of 10-40%.

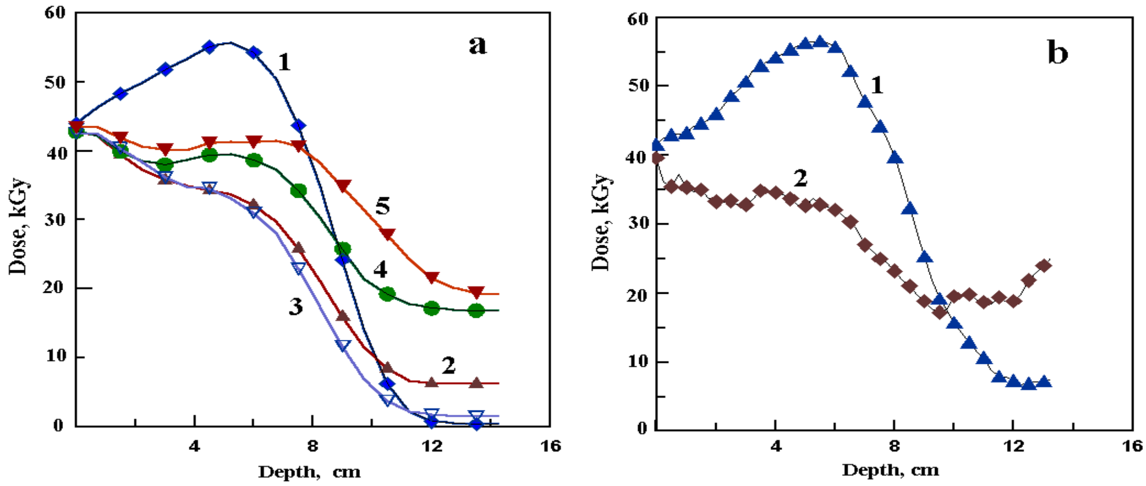

Fig. 13. The depth-dose distributions near the boundary of wooden block with air.

a) Simulation results: 1- depth-dose distribution in homogeneous wooden material; 2 - depth-dose distribution in the wooden block near the boundary with air under inclination angle β = 0 degree; 3 – depth-dose distribution in the wooden block on the left lateral side (shadow side) of target under inclination angle β = 3 degree; 4 - depth-dose distribution in the wooden block on the right lateral side (highlighted side) of target under inclination angle β = 3 degree; 5 - depth-dose distribution in the wooden block near the boundary with air irradiated by electron beam with angular spread of 6 degree under inclination angle of target β = 0 degree.

b) Experimental results: 1 - depth-dose distributions measured in the center of homogeneous wooden material; 2- depth-dose distribution in wooden block near the boundary with air under inclination angle of target β= 0 degree.

Fig 13 (b) represents the results of experimental measurements of the depth-dose distributions near the boundary of wooden block with air. Curve 1 is the depth-dose distributions measured in the center of homogeneous wooden material. Curve 2 represents of the experimental depth-dose distribution in wooden block near the boundary with air under inclination angle of target β = 0 degree. The inclination angle of irradiated target was not controlled precise in time of target movement across an irradiation field. Additional uncertainties in determination of the inclination angle of irradiated target can be appears due to vibration of target on running rollers of conveyer in time of irradiation.

3D-view of the depth-dose distributions near the boundary of wooden block with air at various inclination angles β of the target are presented in Figs. 14(a) and (b): β = 0 degree (Fig. 14(a)) and β=3 degree (Fig. 14(b)). Wooden block is irradiated by scanning electron beam at double-sided.

Results of Monte Carlo simulation and experimental results of the depth-dose distribution near the boundary of Al block with air are presented in Fig.15. Curves 1 and 2 are the depth-dose distributions in center (Curve 1) and near the boundary (Curve 2) of Al block with air. Curves 3 and 4 are experimental results of the depth-dose distributions in distributions in center (Curve 3) and near the boundary (Curve 4) of Al block with air without inclination of Al target (angle β=0 degree). Experimental results for dose distribution were measured by CTA dosimetric film placed on the lateral face of Al block.

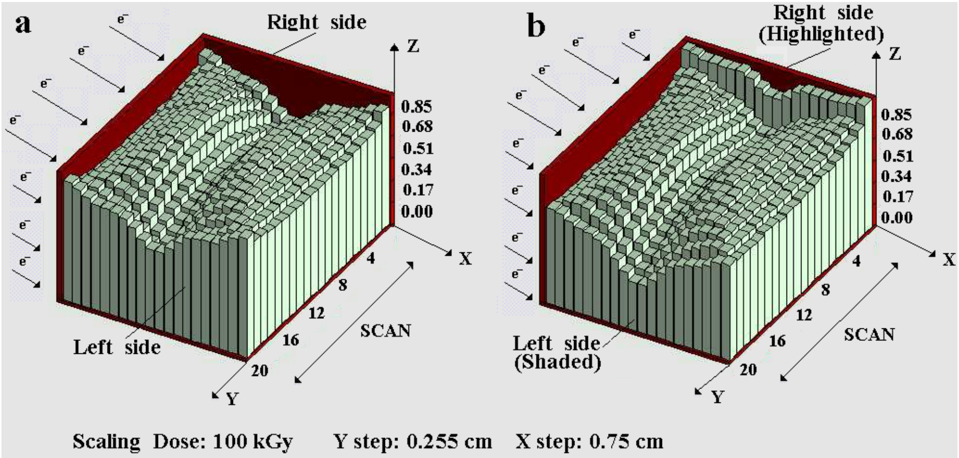

Fig. 14. 3D-view of the dose distribution near the boundary of wooden block with air at different inclination angles β of the target.
a) Inclination angles β = 0 degree. b) Inclination angles β = 3 degree.

As it is seen from Fig. 13(a) and Figs. 14 (a), (b), the depth-dose distributions near the boundary of wooden block with air are very sensitive to orientation of a lateral face of block relatively to axis of electron beam as well as to the angular spread of electron beam. The same results simulation were obtained for the depth-dose distributions near the boundary of Al and PE blocks with air. Such tendency for the depth-dose distribution is typical for boundary of contacting materials with essentially different densities, i.e. $\rho_1 << \rho_2$. As this takes place, the values and shapes of depth-dose distributions on the opposite boundaries of inclination targets are identical for inclination angle β =0 degree (see Fig.14(a)), and can essentially differ for β ≠0 degree (see Fig.14(b)). The visual analysis of the depth-dose distribution on the Figs. 13(a), (b) and Fig.15 demonstrates a satisfactory agreement of the shapes and absolute values of the depth-dose distributions near the boundaries of Al and wooden blocks with air for theoretical predictions and experimental validation.

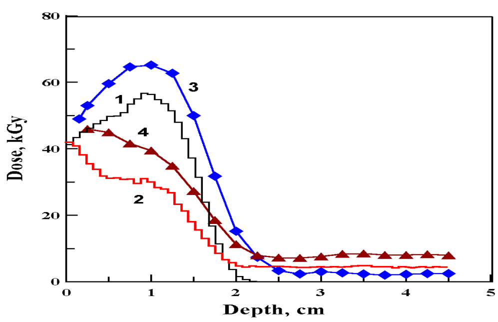

Fig. 15. Simulation and experimental results of depth dose distribution near the boundary of Al block with air:
1, 2 - results of calculations by a method Monte Carlo of the dose distributions at center (1) and near the boundary (2) of Al block with air; 3, 4 - experimental results of the dose distributions at center (3) and near the boundary (4) of Al block with air.

The features of the boundaries effects of contacting materials with essentially different densities are the following: on some thickness of irradiated materials, the value of absorbed dose near the boundary exceed the value of absorbed dose in material with greater density. This effect is very sensitive to orientation of lateral face of irradiated materials relatively to axis of electron beam and to the angular spread of electron beam. The values and shapes of depth-dose distributions on the opposite boundaries of inclination targets are identical for inclination angle β = 0 degree, and can essentially differ for β ≠ 0 degree, even at very small inclination angle β ~ 1 degree.

The sensitivity of the depth-dose distribution to orientation of lateral face of irradiated materials relatively to axis of electron beam and to angular spread of electron beam is determined by a significant influence of the lateral highlight of the scattering electrons in an air on the forming of a dose field on the materials boundary. The lateral highlight of the scattering electrons contribute significantly to the depth-dose distributions along of electron range in an irradiated materials.

For more correct comparison of theoretical predictions with dosimetry for boundaries effects of dose distributions of contacting materials with essentially different densities, it is necessary to have more detailed and accurate information about radiation facility setup, parameters of electron beam, spatial orientation of irradiated target with respect to electron beam axis.

The ModeRTL program allows to determine not only optimum parameters of a mode of an irradiation or to determine optimum setup of dosimetric experiment, but also to determine possible errors for dose distribution, which arise because of uncertainties of various parameters in actual experiment. The program allows to forecast and to calculate necessary accuracy, which it is necessary to set for the good agreement of simulation results and experimental data.

CONCLUSION

Theoretical investigations of boundaries effects of dose distribution at passage of electron irradiation through heterogeneous targets were performed on base of mathematical modeling by ModeRTL software. Basic laws of an electron dose distribution near the boundaries of the contacting materials with different density and/or atomic number were predicted by computer simulation. The experimental and theoretical examinations of boundary anomalies of the absorbed dose distribution were carried out on model samples. Both used materials (Al, PE, wood, CTA film) and radiation facility on the basis of the LAE 13/9 are typical for a series of radiation technologies. An experimental validation of basic laws of boundary effects with dosimetry was confirmed.

It was established, that the boundary anomalies of a dose are always realized at radiation processing of heterogeneous materials in practice. Investigation of those anomalies is necessary to estimation the quality and mass throughput rate of an irradiation process fulfilled on radiation facility. It is shown that an application of designed ModeRTL software for planning of irradiation on RTL, control and execution of irradiation process, and interpretation of dosimetric results is correct and very useful in practical activity.

REFERENCES

1 ASTM Standard 1649-94. Standard practice for dosimetry in an electron beam facility for radiation processing at energies between 300 keV and 25 MeV. Annual Book of ASTM Standards. Vol. 12.02. American Society for Testing and Materials, West Conshohoken, PA 19428, USA.

2. Lazurik V.T., Lazurik V.M., Popov G.F., Rogov Yu.V. Software tools for optimization of industrial EB and X-ray processing. Proceedings of the 7-th Intern. Conference on Electron Beam Technologies, EBT 2003. Varna, Bulgaria. -2003.- P. 616-622.

3. Kaluska I., Lazurik V.T., Lazurik V.M., Popov G., Rogov Yu.V., Zimek Z. Dose distribution in the heterogeneous materials irradiated by electron beams. Abstract book of the XVIII International Workshop on Charged Particle Accelerators. Alushta, Ukraine. - 2003.- P. 209-210.

4. Okuda S., Fukuda K., Tabata T. and Okabe S. Influence of a dye film dosimeter inserted in a solid on electron behavior and dosimetry //Nuclear Instruments and Methods.-1982.- V.200. - P.443-447.

5. Lazurik V.T., Lazurik V.M., Popov G.F., Rogov Yu.V. Integration of simulation methods in control system for EB processing. Proceedings of the Phys.Con 2003 Conference. Saint Petersburg, Russia. - 2003.- P.1003-1008.

6. Lazurik V.T., Lazurik V.M., Popov G.F. and Rogov Yu.V. Modeling of processes of an irradiation for industrial technologies. Bulletin of the Kharkiv National University, Series "Mathematical modeling. Information technologies. Automatic control systems". – 2003, N 605.- Issue 2.- P.72-89.

7. Zimek Z., Kołyga S., Levin V.M., Nikolaev V.M., Rumyantsev V.V., Fomin L.P. An Institute of Nuclear Research Electron Linac, Nukleonika. - 1972. – **17**, 1-2. - P. 67-75.

8. ICRU, Stopping powers for electrons and positrons. ICRU Report 37, Bethesda, MD. - 1984.

9. Bielajew A.F., Rogers D.W. and. Nahum A.E. The Monte Carlo simulation of ion chamber response to ^{60}Co resolution of anomalies associated with interfaces.// Phys. Med. Biol.- 1985.- V. 30, N 5. - P. 419-427.

ОСНОВНЫЕ ЗАКОНОМЕРНОСТИ ГРАНИЧНЫХ ЭФФЕКТОВ ДЛЯ РАСПРЕДЕЛЕНИЯ ПОГЛОЩЕННОЙ ДОЗЫ ЭЛЕКТРОНОВ В ГЕТЕРОГЕННЫХ МАТЕРИАЛАХ

И. Калуска[**], В.Т. Лазурик [*], В.М. Лазурик[*], Г.Ф. Попов[*], Ю.В. Рогов[*], З. Зимек[**]

[*] *Харьковский Национальный Университет им В.Н. Каразина, Харьков, Украина*

[**] *Институт Ядерной Химии и Технологии, Варшава, Польша*

Аномалии распределения поглощенной дозы (РПД) электронов на границе раздела контактирующих материалов при ориентации границы параллельно падающему пучку электронов были предсказаны компьютерным моделированием программой ModeRTL. Экспериментальная проверка правильности теоретических предсказаний проведена на радиационно-технологической линии. Гетерогенные мишени облучали сканирующим пучком электронов с энергией 10 МэВ на движущемся конвейере. Предсказанные моделированием общие закономерности поведения РПД на границе раздела материалов с различными плотностями и/или атомными номерами подтверждены экспериментально. Рассматриваются физические модели для объяснения наблюдаемых граничных эффектов.

КЛЮЧЕВЫЕ СЛОВА: поглощенная доза, пучок электронов, граничные эффекты, моделирование, экспериментальная проверка